

**Theoretical and X-ray studies on the cyclization of 1-phenyl-5-(3-aryltriaz-1-en-1-yl)-1H-pyrazole-4-carbonitriles and 2-amino-3-(3-aryltriaz-1-en-1-yl)maleonitriles:
A comparison study**

Amal Al-Azmi^{1,*}, Firas F. Awwadi²

¹*Dept. of Chemistry, Kuwait University, P. O. Box 5969, Safat 13060, Kuwait*

²*Dept. of Chemistry, The University of Jordan, Amman 11942, Jordan*

**Corresponding author: amalrchem@gmail.com*

Abstract

The present work investigates attempts to cyclize 1-phenyl-5-(3-aryltriaz-1-en-1-yl)-1H-pyrazole-4-carbonitriles to the desired pyrazolo[3,4-*d*] [1,2,3] triazinimine derivatives. The cyclizations were unfruitful, and a density functional theory study was performed. This revealed that 1-phenyl-5-(3-aryltriaz-1-en-1-yl)-1H-pyrazole-4-carbonitriles are more stable than the targeted pyrazolo[3,4-*d*][1,2,3]triazinimine derivatives, indicating that their cyclization is thermodynamically disfavoured; the reactant 8c is more stable than the predicted six-membered ring products 9c by 5 kJ/mol. The effect of isomerization of the methoxy-phenyl group in the self-assembly of 8c and 8d in the crystalline lattice was investigated. The intermolecular forces in the solid-state were analyzed for the two structural isomers 8c and 8d using calculated Hirsh Feld surface; the analysis indicates that the intermolecular forces are stronger in 8c than 8d and hence 8c is denser than 8d by 0.071g/mL.

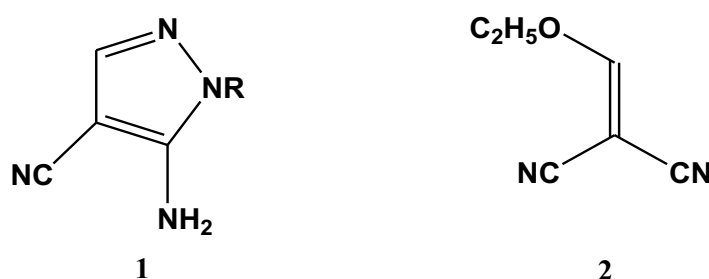
Keywords: Cyclization; density functional theory (DFT); diazotization; N-heterocycles; Pyrazoles

1. Introduction

Pyrazoles are a well-known class of five-membered ring heterocycles containing two vicinal nitrogen atoms (Al-Azmi, 2019, Kumar & Jayaroopa. 2013), they are also known as 1,2 diazoles. They become famous because of their various uses. Many pyrazole derivatives have a wide range of biological activities, this accelerated the research activity in several fields, especially the biological field. Among these pyrazoles is 5-aminopyrazole-4-carbonitrile derivatives 1 which contain both reactive NH₂ and CN functional groups. In recent years, the synthesis of these compounds has received increased attention due to their significant role in the pharmaceutical industry (Al-Azmi, 2019, Kumar & Jayaroopa. 2013). This was the driving force to synthesize a wide range of 5-aminopyrazole-4-carbonitriles 1 along with different substituents. 5-Aminopyrazole-4-carbonitriles 1 is usually synthesised from 2-ethoxymaleonitrile 2. Current research has focused mainly on utilizing both NH₂ and CN

groups in several chemical conversions, which has led to the synthesis of various pyrazoles containing compounds.

Numerous pyrazoles have shown antibacterial, anti-inflammatory, anti-tubercular, anti-cancer activities, anti-convulsant, anti-microbial, anti-diabetic, and also anti-cancer activities (Al-Azmi 2019, Kumar & Jayaropa 2013, Al-Azmi & Mahmoud 2020). Other derivatives have been evaluated for their analgesic and sedative effects. In addition, a group of 5-chloro-1-phenyl-3-methylpyrazolo-4-methinethiosemicarbazanes has been described as corrosion inhibitors for carbon steel (Abdelhamid *et. al.* 2016, Arrousse *et.al* 2020, El-Hajjaji, *et. al.* 2018).



In this manuscript, we are exploring two different cyclization routes which lead to five-membered rings and six-membered rings theoretically. This is supported by the x-ray crystal structures of 8c and 8d and they are rationalized.

2. Results and discussion

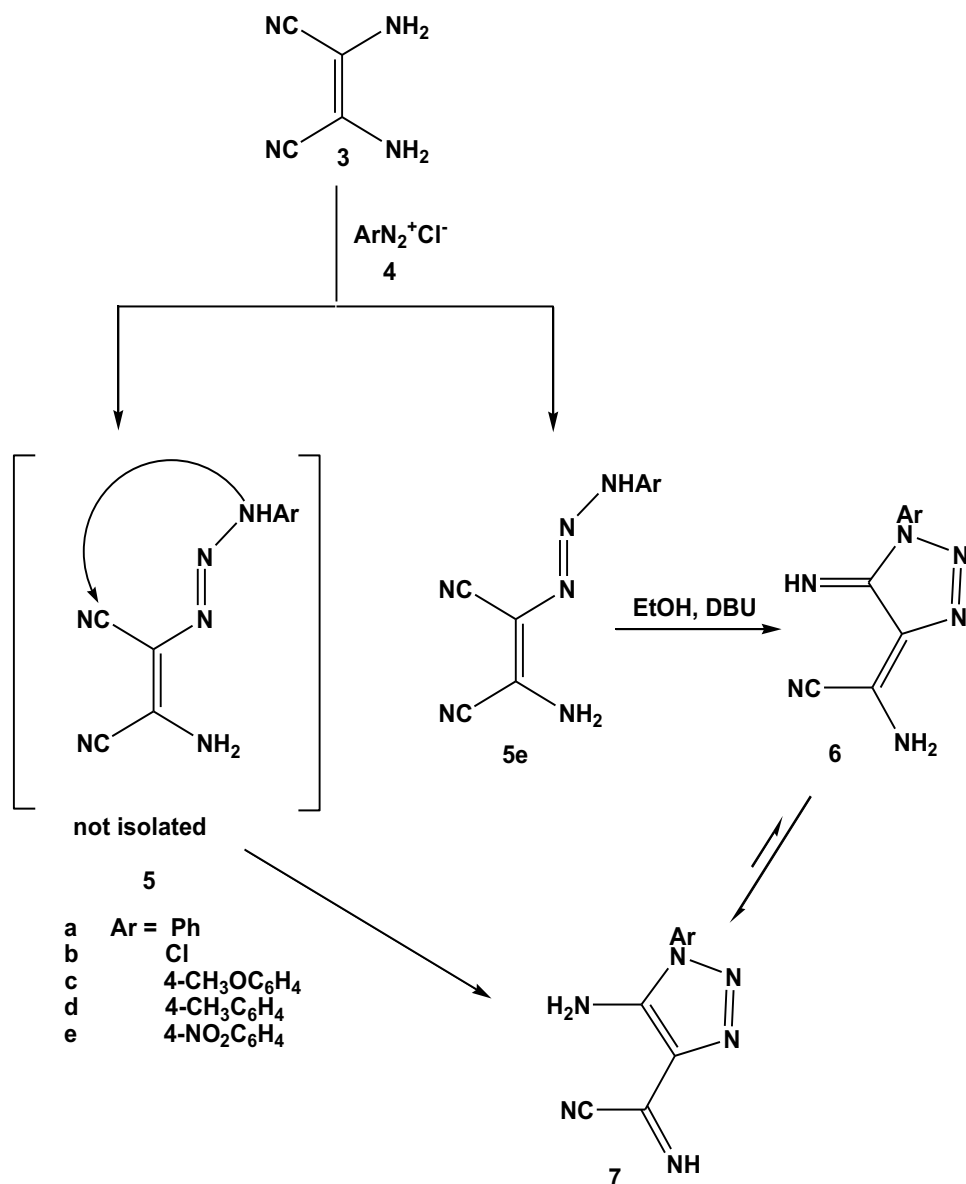
In 2013, we reported that the reaction of diaminomaleonitrile (DAMN) 3 with aryl diazonium salts 4 ($Ar \neq NO_2C_6H_4$) furnished triazoles 7 *via* the attack of the NH function on the electrophilic carbon of the CN group (Al-Azmi & Kalarikkal 2013) (Scheme 1).

With 4-nitrophenyl diazonium salt, however, the intermediate 5e prior to cyclization was isolated and fully characterized. The isolation was attributed to the strong electron-withdrawing effect of the nitro group, which reduced the nucleophilicity of the -NH. Further, cyclization to the desired triazole 7e ($Ar = NO_2C_6H_4$) was successfully achieved when a catalytic amount of 1,8-Diazabicyclo [5.4.0] undec-7-ene (DBU) was added to the isolated intermediate in the presence of ethanol as a solvent.

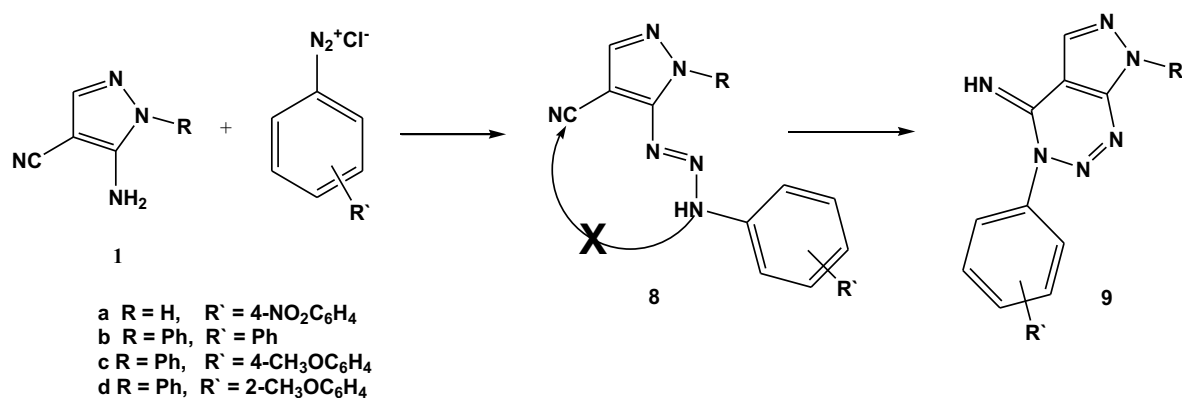
The synthesis of compound 8 was reported previously by our group in investigating new pyrazole derivatives as antimicrobial compounds (Al-Azmi & Mahmoud 2020). We found that they have intermediate activity towards several microbes.

When the nitro derivative was isolated instead of the expected six-membered ring (Al-Azmi & Shalaby 2018), it was attributed to the electron-withdrawing effect of the nitro group (*vide supra*), (Al-Azmi & Kalarikkal 2013) and attempts to cyclize it using ethanol and a catalytic amount of DBU were aborted. It was expected that if the nitro group is replaced by electron-donating substituents, cyclization will proceed, and pyrazolo[3,4-*d*] [1,2,3] triazinimines 9 will

be formed instantly Scheme 2. However, this was not achieved, and pyrazoles 8 were recovered. Several trials to cyclize the corresponding compounds utilizing various conditions, including different polar and non-polar solvents, and various bases, such as Et₃N, pyridine, and NH₃, at various temperatures, were ineffective. The cause is inconclusive. Consequently, density functional theory (DFT) calculations were carried out to determine the reason behind such behavior.



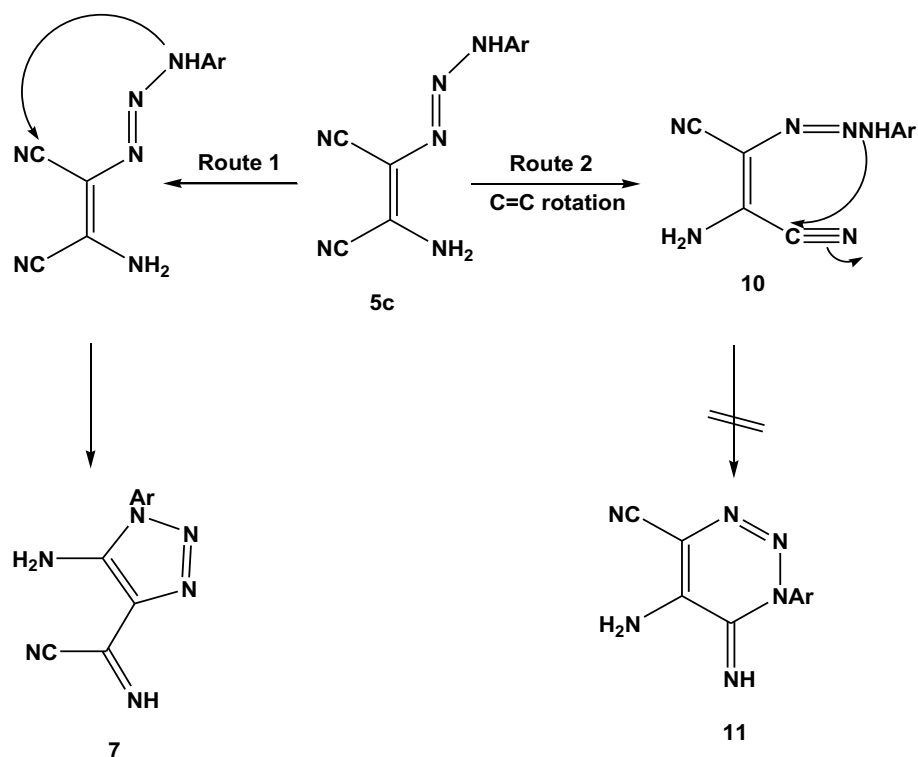
Scheme 1.



Scheme 2.

3. Density Functional Theory Study

Two compounds were studied for comparison 5 and 8 to understand why compound 8 is not cyclized and to discover the required factors to facilitate the cyclization process. Two pathways of cyclization of 5c are possible: a five-membered ring 7 as shown in *route 1* or a six-membered ring 11 as shown in *route 2*; see Scheme 3.



Scheme 3.

Experimentally, only *route 1* was observed, as P1 was experimentally isolated and characterized (Al-Azmi & Kalarikkal 2013). Two conformers of 5 (Ar = CH₃OC₆H₄) were optimized (R1 and R2); R1 is found to be more stable than R2 by 8.9 kJ/mol; see Figure 1. The extra stability is due to the N-H...N hydrogen bonding interactions. Although P2 is more stable than P1 by 20 kJ/mol, P2 was not isolated. This is mainly because of the shorter N1...C1 distance (4.496 Å, Figure 4) compared to the N1...C2 distance (5.546 Å, Figure 2). The rotation around C=C double bonds is not feasible due to the high-energy barrier associated with rotation (182.4 kJ/mol, Figures S1, S2, and S3), which rules out the formation of P2, as observed. The rotation around the N-N single bond is more probable because it is associated with average energy barriers of TS1 and TS2 of 76.2 kJ/mol (Figure S3). TS2 is less important to our discussion, as the nitrile groups are in *trans* arrangement, and the rotation around the C=C double bond is kinetically disfavoured. Even though the energy barrier associated with TS1 (71.1 kJ/mol) is significantly lower than that associated with TS3, it is still considered a high-energy barrier. In addition, R3 is less stable than R1 by 15 kJ/mol (Figure S3). This agrees with the formation of P1, as observed experimentally.

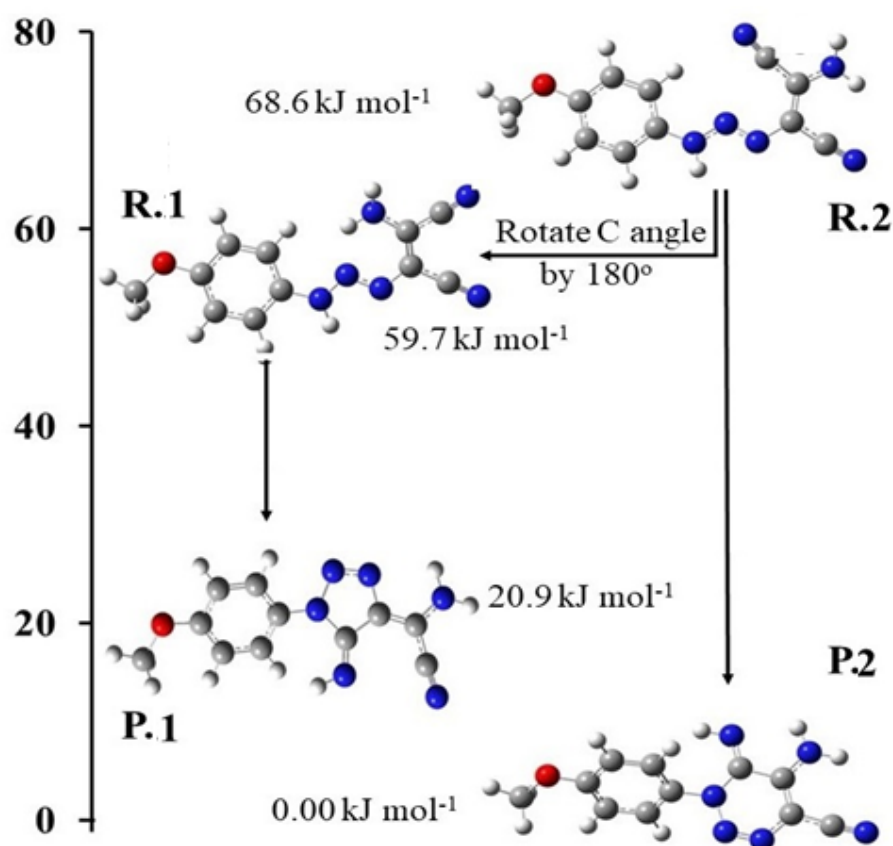


Fig. 1. Relative energies of R.1, R.2, P.1, and P.2.

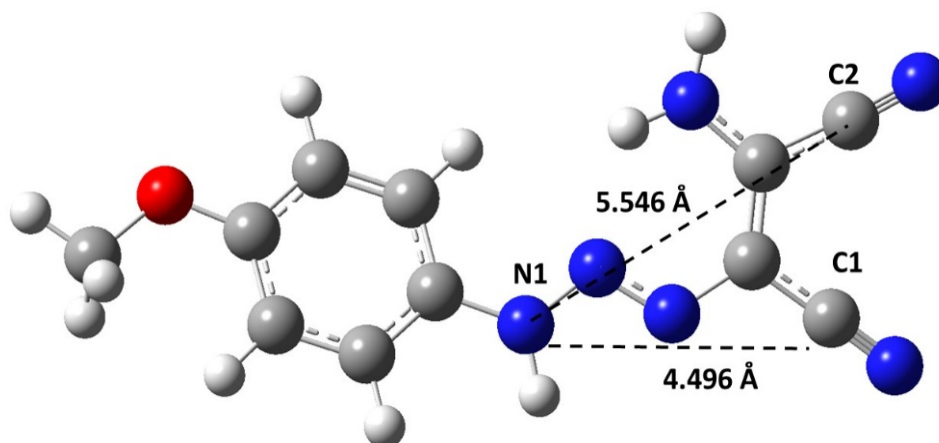


Fig. 2. The optimized structure of compound 5c.

The calculations were repeated using different organic substituents in the para position of the benzene ring. The data are summarised in Table 1. R1 (*Cis* isomer) is always more stable than R2 (*Trans* isomer). Similarly, P2 is always more stable than P1 (Table 1), for example when R= OCH₃, P2 is more stable than P1 by 20.9 kJ/mol.

Table 1. Relative energies of R1, R2, P1, and P2 (Figure 3). For each R substituent, the energy of P2 is set as a reference and given the value of zero to calculate the relative energy.

R - subs	Reactant	Relative Energy in kJ mol ⁻¹	Product	Relative Energy in kJ mol ⁻¹
OCH ₃	R2	68.6	P2	0.0
	R1	59.7	P1	20.9
CH ₃	R2	65.1	P2	0.0
	R1	56.1	P1	19.4
H	R2	63.5	P2	0.0
	R1	54.6	P1	18.7
Cl	R2	62.3	P2	0.0
	R1	55.1	P1	17.8

In the case of pyrazole derivatives 8, the possibility of forming a five-membered ring was ruled out by having only one nitrile group, which may lead only to the formation of six-membered ring derivatives 9. However, the desired pyrazolo[3,4-*d*][1,2,3]triazinimines 9 were not isolated. Optimizing of the reactant 8c and the predicted six-membered ring products 9c (Figure 3) shows the formation of the six-membered ring pyrazolo[3,4-*d*][1,2,3]triazinimine 9c is actually disfavoured thermodynamically. The reactant 8c proved to be more stable than the six-membered ring 9 product by 5 kJ/mol.

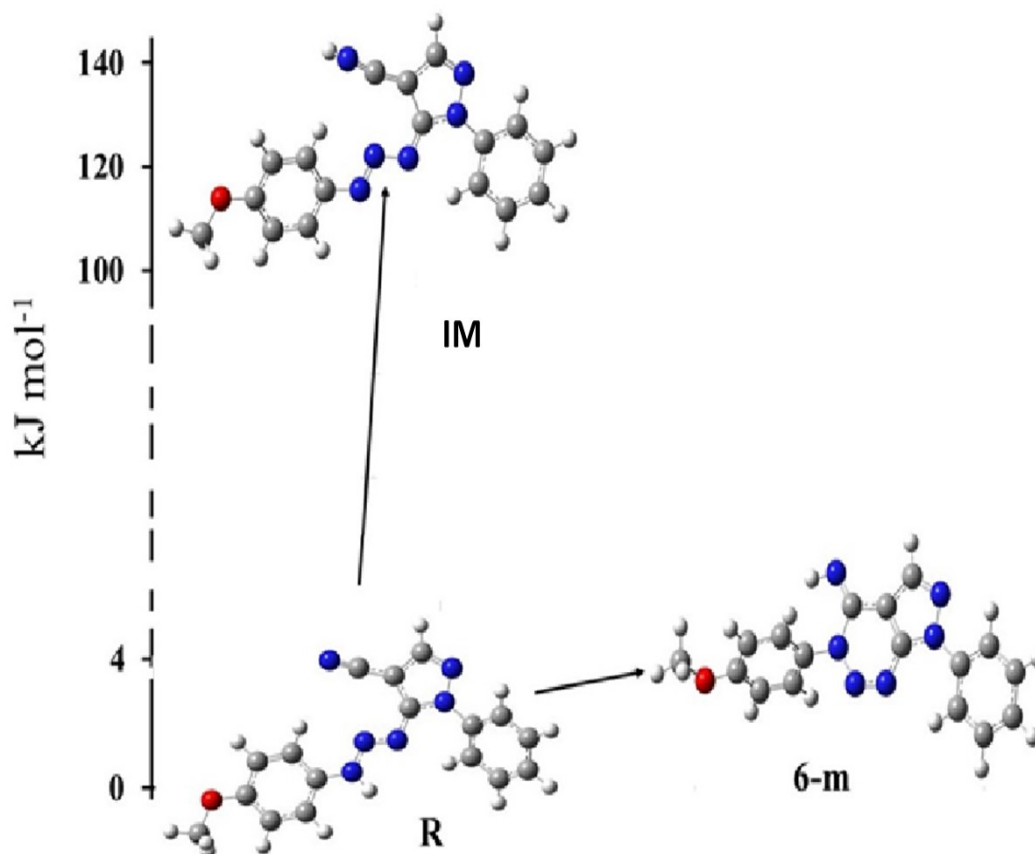


Fig. 3. The relative energies of the reactant, intermediate and six-membered ring product.

The crystal structures of 8c and 8d (CCDC 1967744, CCDC 1967745) (Figures 4 and 5) were determined at room temperature. (Tables S1-S5) Apparently, there is an interaction between N5 and C10; the N5...C10 inter-nuclear distances are 2.849(2) Å and 2.910(3) Å in 8c and 8d, which are less than the sum of van der Waals by 0.4 Å and 0.34 Å. The result is that the atoms (N4, N5, C8, C9, and C10) are coplanar; the root-mean-square deviation (RMSD) from the mean plane of the mentioned atoms is 0.043 Å and 0.031 Å in 8c and 8d. Intermolecular interactions between nucleophilic atoms and electron-deficient carbon atoms have been observed in the literature (Braga 2009, Sammor *et. al*, 2018). The phenyl ring (C1-C2-C3-C4-C5-C6) is nearly perpendicular to the plane of the five-membered ring in 8d, whereas it is tilted in 8c; the angles between the phenyl ring and the five-membered ring are 84.0 (1)° and 39.26(9)° in both 8c and 8d. This is due to the presence of the methoxy group in the *ortho* position in pyrazole 8d; there is an intra-molecular N6-H...O1 hydrogen bond. Therefore, the methoxy group in the *para* position in 8c allows the formation of N6-H...N2 inter-molecular hydrogen bonding interactions, as shown in Figure 6. Therefore, this forces the phenyl ring to be nearly perpendicular to the five-membered ring.

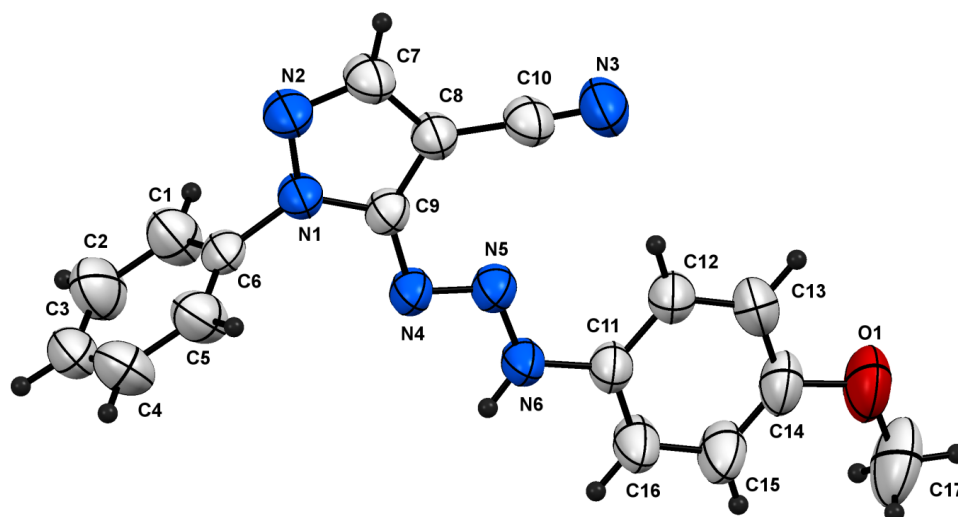


Fig. 4. X-ray crystallographic data was determined for compound 8c.

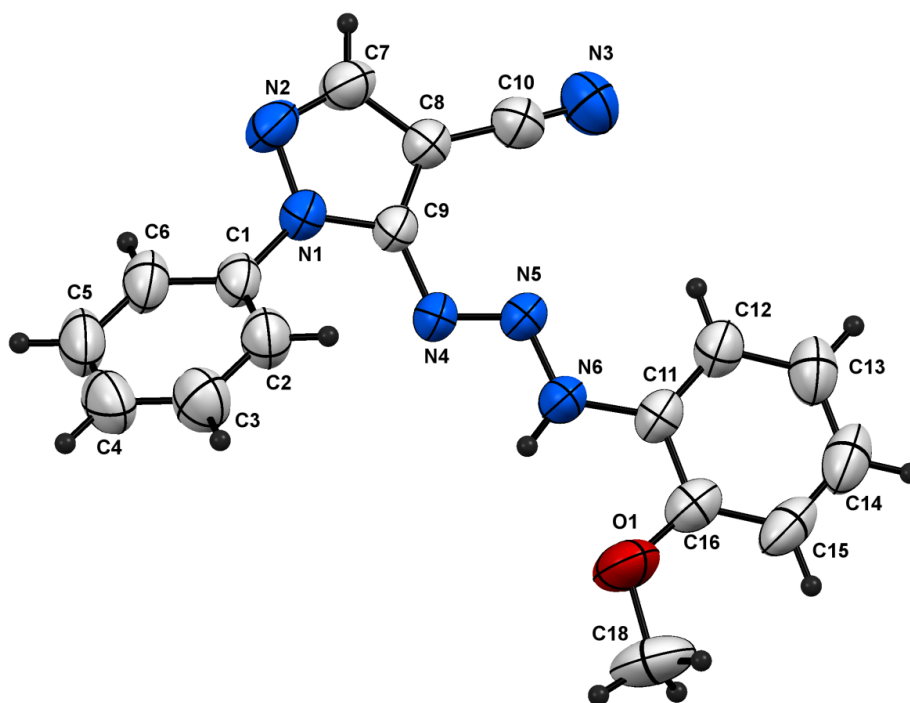


Fig. 5. X-ray crystallographic data was determined for compound 8d.

The Hirshfeld surface (Figure 6) was used to analyze the intermolecular forces and thus the supramolecular structure. The surface analysis indicates there are N-H...N and C-H...N hydrogen bonding interactions and C-H... π interactions in 8c, whereas there are only C-H...N interactions in 8d. The data summarising these interactions are listed in Table 2. The data indicates the interactions are more robust in 8c than in 8d; therefore, 8c is denser than 8d by 0.071g/mL. (Table S5) Similar intermolecular interactions to that presented in 8c were observed in the analog of 8c and 8d, where the methoxy group is replaced by hydrogen (Al-

Azmi & Mahmoud 2020). Stronger N-H...N hydrogen bonding interactions with the aid of C16-H... π interactions connect the molecular units of 8c to form chain structures that run parallel to the *b*-crystallographic axis (Figure 7). Subsequently, the chains form a three-dimensional structure via weaker interactions (Table 2 and Figure 7). The C5-H...N3 interactions link the molecular units of 8d to form chain structures that run in a parallel [110] crystallographic direction (Table 2 and Figure 8).

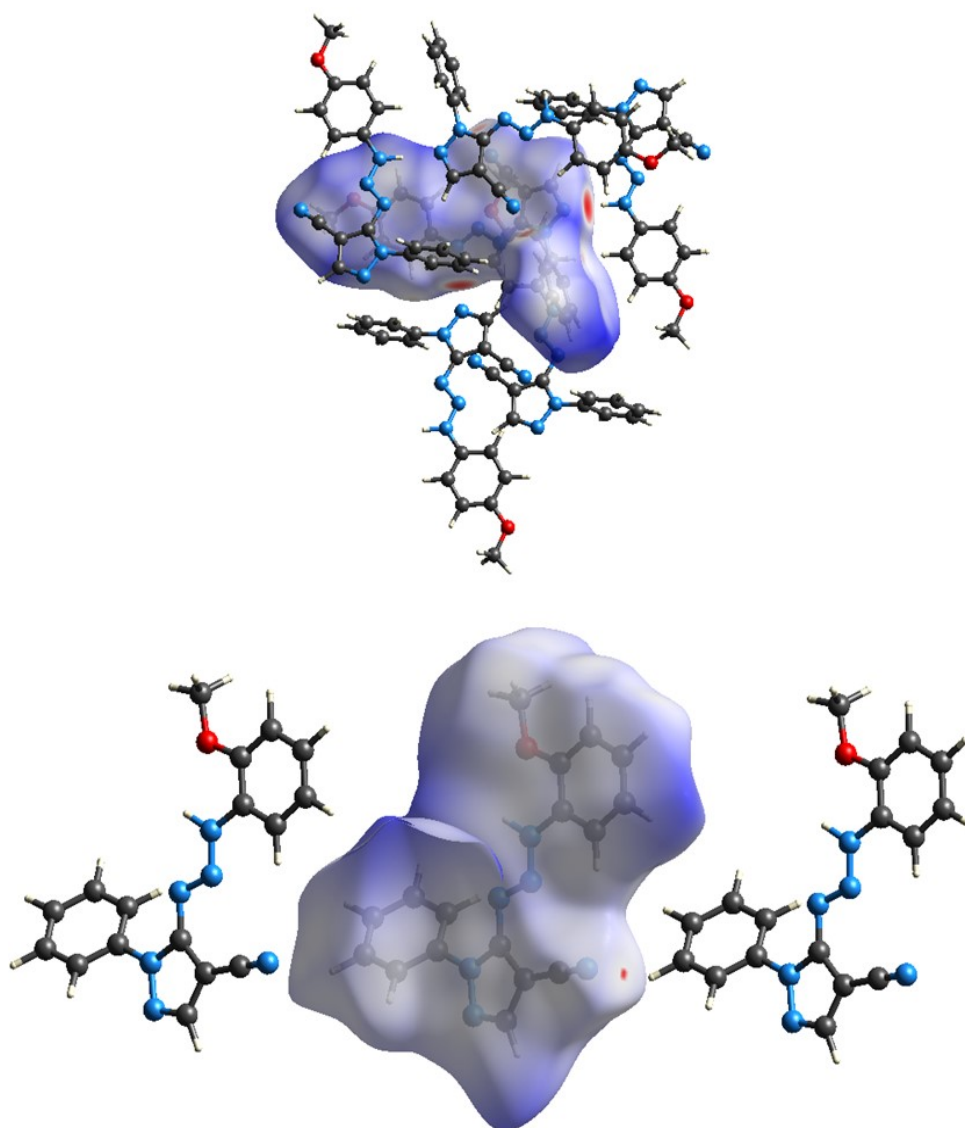


Fig. 6. Hirshfeld surface and illustration of intermolecular forces in 8c (top) and 8d (bottom). The plots were generated using CrystalExplorer (Turner *et. al.* 2017)

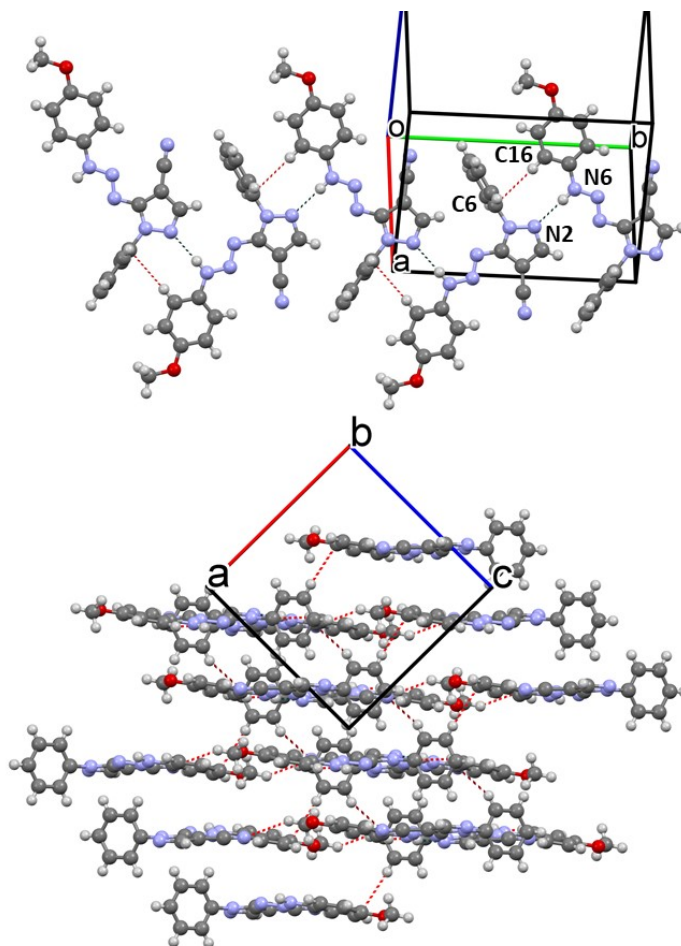


Fig. 7. The chain structure of compound 8c (top) and its three-dimensional structure (bottom) are viewed from the b-axis. The stronger N-H...N hydrogen bonding interactions are represented by black dotted lines, and the other weaker interactions are represented by red dotted lines (Table 2).

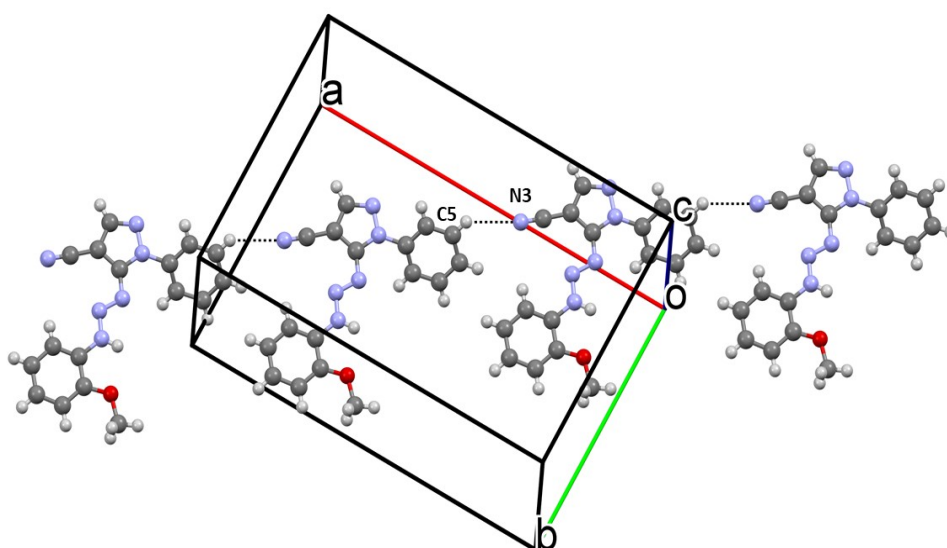


Fig. 8. Illustration of chain structure in 8d.

Table 2. D-H...An interaction distances (Å) and angles (°) in 8c and 8d.

8c			
D-H...A	D...A	H...A	D-H...A
N6-H...N2 ⁱ	2.971(2)	2.126(2)	167.2(1)
C17-H...N3 ⁱⁱ	3.554(4)	2.725(2)	144.9(2)
C1-H...N3 ⁱⁱⁱ	3.404(3)	2.528(2)	157.1(1)
C16-H... $\pi^{a, i}$	3.745(3)	2.838(2)	165.1(1)
^b C2-H... π^{iv}	3.656(3)	2.888(2)	140.8(2)
8d			
C5-H...N3 ^v	3.824(2)	2.699(2)	169.8(2)

The listed distances and angles are to the closest carbon atom in the π system (C6).

^b The listed distances and angles are to the closest carbon atom in the π system (C14).

Symmetry transformations used to generate equivalent atoms: ⁱ2-x, -0.5+y, 0.5-z; 1-x, -0.5+y, 1.5-z; ⁱⁱⁱ 2-x, 2-y, 1-z; ^{iv} 1+x, ^v 1.5-y, -0.5+z; ^v -0.5+x, -0.5+y, z.

4. Experimental

The synthesis and spectroscopic analyses of the compounds 5c (Al-Azmi & Kalarikkal 2013) and 8c (Al-Azmi & Mahmoud 2020) studied in this work were previously described.

The single-crystal X-ray diffraction analysis of the crystal samples was made by Rigaku R-Axis RAPID diffractometer using filtered Mo-K α radiation at 293K. The data collection was carried out using 'Crystalclear' (Rigaku, Japan) and data processing was done by 'CrystalStructure' (Rigaku, Japan) software packages. Finally, the structure refinement of these crystals was performed by SHELXL - 2017/1. During structure refinement, non-hydrogen atoms were refined anisotropically, whereas all hydrogen atoms were assigned at calculated positions and were refined using the riding model. All optimization calculations were carried out using G09 at the DFT/Becke, 3-parameter, Lee–Yang–Parr (B3LYP) level (Becke, 1988) cc-pvtz basis sets were assigned for all atoms. The transition state was estimated using the synchronous transit-guided quasi-Newton method (Gaussian keyword = QST2).

5. Conclusion

This work demonstrates that pyrazolotrizimines are stable and cannot be cyclized to the expected pyrazolo[3,4-*d*][1,2,3]triazinimines. DFT calculations revealed that their formation is thermodynamically disfavoured in terms of energy. The fact that 8c is denser than 8d was determined using intermolecular force; the intermolecular force in 8c is stronger than in 8d. Due to the skeletal isomerization of the two compounds, the methoxy group is in the *ortho* position in 8d, whereas it is in the *para* position in 8c.

ACKNOWLEDGMENTS

Financial support from Kuwait University was received through research grant SC 04/19. We gratefully acknowledge the Research Sector Project Unit (RSPU)- Kuwait University facilities through projects GS 01/01, GS 01/03, GS 03/08, and GS 01/05.

References

A. Al-Azmi. (2019). Pyrazolo[1,5-*a*]pyrimidines: A Close Look into Their Synthesis and Applications. *Current Organic Chemistry*, **23**, 721-743.

<http://dx.doi.org/10.2174/1385272823666190410145238>.

Al-Azmi, A. & Mahmoud, H. (2020). Facile Synthesis and Antimicrobial Activities of Novel 1,4-Bis(3,5-dialkyl-4*H*-1,2,4-triazol-4-yl)benzene and 5-Aryltriaz-1-en-1-yl-1phenyl-1*H*-pyrazole-4- carbonitrile Derivatives, *ACS Omega*, doi.org/10.1021/acsomega.0c01001.

Al-Azmi, A. & Kalarikkal, A. K. (2013). Synthesis of 1,4,5-trisubstituted-1,2,3-triazoles *via* a coupling reaction of diaminomaleonitrile with aromatic diazonium salts. *Tetrahedron*, **69 (52)**, 11122-11129. <https://doi.org/10.1016/j.tet.2013.11.003>.

Al-Azmi, A. & Shalaby, M. A., (2018). Experimental and computational approaches to the analysis of the molecular structure of (*E*)-3-(3-(4-nitrophenyl)triaz-1-en-1-yl)-1*H*-pyrazole-4-carbonitrile. *J. Mol. Struct.*, **1155 (5)**, 239-248. <https://doi.org/10.1016/j.molstruc.2017.11.006>.

Abdelhamid, A. O., El-Idreesy, T. T., Abdelriheem, N. A., & Dawoud. H.R.M., (2016). Green One-Pot Solvent-Free Synthesis of Pyrazolo[1,5-*a*] pyrimidines, Azolo[3,4-*d*]pyridiazines, and Thieno[2,3-*b*]pyridines Containing Triazole Moiety. *J. Heterocycl. Chem.*, **53**, 710-718. <https://doi.org/10.1002/jhet.2343>.

Arrousse et.al (2020). "The inhibition behavior of two pyrimidine-pyrazole derivatives against corrosion in hydrochloric solution: Experimental, surface analysis and in silico approach studies". *Arab. J. Chem.*, **13 (7)**, 5949-5965. doi.org/10.1016/j.arabjc.2020.04.030.

Becke A. D. (1988). Density-functional exchange-energy approximation with correct asymptotic behavior. *Phys. Rev. A.*, **38 (6)**, 3098-3100. doi:10.1103/PhysRevA.38.3098.

Braga, D., Grepioni, F., Maini, L. & Polito, M. (2009). Crystal Polymorphism and Multiple Crystal Forms. *Struct. Bonding*, **132**, 25–50. DOI:10.1007/430 2008 7.

Crystallographic data of **8c** have been deposited with the Cambridge crystallographic data center as supplementary publication number **CCDC 1967744**.

Crystallographic data of **8d** have been deposited with the Cambridge crystallographic data center as supplementary publication number **CCDC 1967745**.

El-Hajjaji, et. al. (2018). Corrosion Resistance of Mild Steel Coated with Organic Material Containing Pyrazole Moiety. *Coatings*, **8 (10)**, 330-346. doi.org/10.3390/coatings8100330.

Kumar, K. A. & Jayaroopa, P. (2013). Pyrazoles: Synthetic Strategies and Their Pharmaceutical Applications-An Overview. *Intern. J. Pharm. Tech. Res.*, **5 (4)**, 1473-1486.

Sammor, M. S., El-Abadelah, M. M., Hussein, A. Q. F., Awwadi, F., Sabri, S. S. & Voelter, W. (2018). A study on the reaction of 3-alkyl(aryl)imidazo[1,5-*a*]pyridines with ninhydrin. *Zeitschrift für Naturforschung B*, **73**, 413-421. <https://doi.org/10.1515/znb-2018-0039>.

Turner, M. J., McKinnon, J. J., Wolff, S. K. Grimwood, D. J., Spackman, Jayatilaka, P. R. D. & Spackman, M. A. (2017). *CrystalExplorer17*. The University of Western Australia. <https://hirshfeldsurface.net>.

Submitted: 01/06/2021
Revised: 19/08/2021
Accepted: 25/09/2021
DOI: 10.48129/kjs.14503